

## Midterm Report: Soft Robotic Fish via Beam Model

Jiajin Cui

### I. PROBLEM AND MOTIVATION

Soft robotic fishes are important in terms of underwater exploration. Although rigid propellers have been widely used nowadays, they generate unwanted noises and turbulent flow. However, flexible robotic fish can adapt to the fluid forces, providing a safer and quieter actuation. However, the complex relationship between the stiffness, actuation frequency, and effectiveness has been an unsolved problem. This project focuses on modeling the robotic fish as a flexible node-spring network to simulate how different key parameters affect the bending behavior.

### II. BACKGROUND AND LITERATURE REVIEW

#### A. Finite-Element-Based Structure Modeling

Katzshman et al. (2018) brought up the idea of robotic fish ‘SoFi. In the paper, he demonstrated a modeling of underwater exploration using different materials and finite element analysis. Their work described the process starting from design to a control planner and testing under water at depths around 18 meters. Utilizing the water-driven actuators, the robot produces motions very similar to a biological fish. The application of a modern modem allows the robot to accept commands such as adjusting speed, angles and depth. Their experiments have shown the capacity of the fish to swim in three dimensions while maintaining low disturbance and noise level. Their physical modeling emphasizes complex hardware design and FEA-based modeling, which extensively increases the complexity of the robot tail.

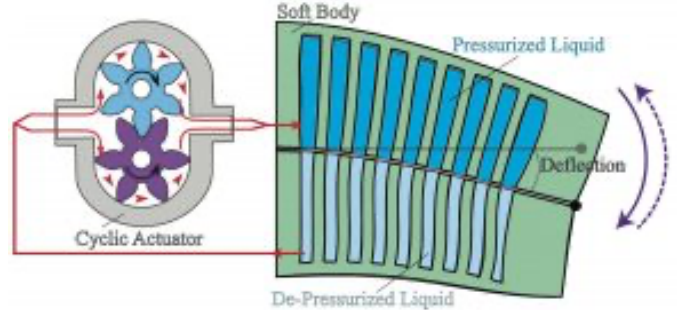


Figure 1: The Internal Structure of A Robotic Fish

#### B. Stiffness, Actuation Frequency and Locomotor Thrust

Esposito et al. (2012), on the other hand, focused on the study of stiffness and actuation of the soft robot fins. They have revealed a strong relationship between stiffness and thrust effectiveness. They work showcased a robotic fish inspired by a bluegill sunfish, with six fin rays being individually actuated. This also enables their fish to be able to swim in three dimensions. They have adjusted parameters such as fin-ray stiffness, flapping frequency, motion control programs studied from biological fish. They have applied sensors to measure forces to show that different values of stiffness produce different thrusts, while the intermediate stiffness produced the largest thrust. They have provided evidence that stiffness is a key variable that determines the locomotor performance.

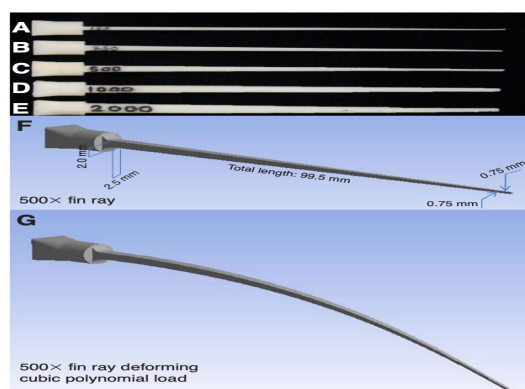


Figure 2 Tails of Different Stiffness

### C. Adjustable Stiffness

In one of the recent papers by Zhong et al. (2021), the team has shown that swimming efficiency highly depends on stiffness of the material by applying tunable stiffness. The team has combined a biomechanical model of a tuna tail and a robotic setup where stiffness can be adjusted to study the relationship between swimming efficiency and tail stiffness. Their study shows that the tail stiffness, representing muscle tension in biological term, should be linearly scaled with the square of swimming speed. They have shown that swimming efficiency could be doubled by finding the ideal stiffness compared to a fixed-stiffness design given certain frequency and speed range. The purpose of the paper is to address the importance of adjust stiffness for different operation conditions.

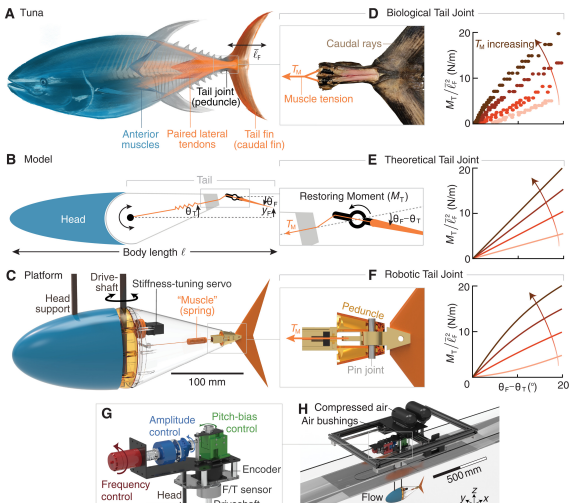


Figure 3 Tuna-based Actuation System

### D. Multiphase Hydrodynamics on Various Platforms

Lauder's team has developed various fish-like robotics and conducted hydrodynamic experiments. They have utilized multiphase hydrodynamics, plastic foils and fish bodies actuated at the leading edge to reproduce the undulatory swimming. Force sensors and flow visualization are also used to determine thrust and efficiency. With all these individual models, the team was able to conduct independent control of different parameters including body length, stiffness, etc. to determine how different deformation, fin shape influence the propulsive force. However, the coupling of a deformable structure and realistic hydrodynamics makes the whole simulation computationally expensive very quickly.

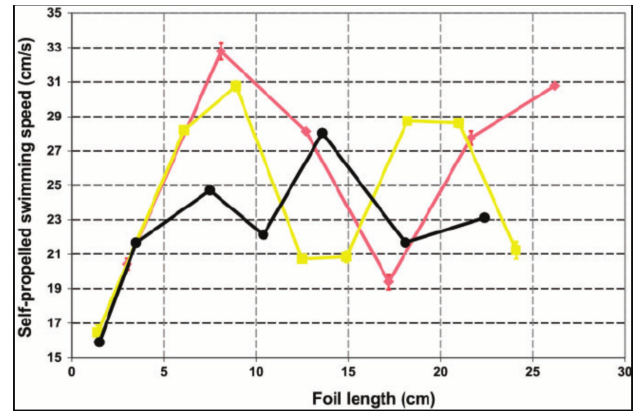


Figure 4 Swimming Speed vs Foil Length

### E. The Optimal Strouhal Number

Eloy (2012) has studied the Strouhal Number for swimming animals. The Strouhal Number is defined as  $St = f/A/U$ , where  $f$  is the tail actuating frequency,  $A$  is the oscillation amplitude, and  $U$  is the swimming speed of the fish. With Lighthill's elongated-body theory, the team has calculated how the optimal Strouhal number for propulsive efficiency depends on the size, and other kinematic parameters by studying over 53 different aquatic species. They have discovered the optimal range of the number for most species they studied to be around 0.2-0.4. The purpose of the study is to provide an interpretation of the swimming efficiency of the natural species, which is a Strouhal number within 0.2-0.4.

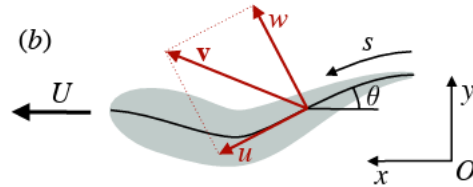


Figure 5 The Decomposition of a Velocity Vector

These prior works have implemented complex analysis/modelling of the soft fin behaviors. They have utilized different sophisticated frameworks such as fluid-structure interaction, computational fluid mechanics, etc. They demonstrate different designs such as tunable stiffness, optimal stiffness distribution and actuation frequency, etc. are essential to swimming efficiency. However, most such studies require heavy computation for multiple experimental platforms or coupled fluid-structure simulations involving Finite Element Analysis and Computational Fluid Dynamics. Considering the scope of this course, this project will model the soft robotic fish an Euler-Bernoulli beam discretized into a node-spring network actuated by curvature as a function of time along the body other than explicit loads. This simplified

framework will isolate key parameters such as stiffness, actuation amplitude, and frequency and study how they affect the pattern and bending deformation of the fish.

### III. PROPOSED APPROACH

This project models the soft robotic fish as a classic Euler-Bernoulli beam with bending stiffness. Actuation will be represented by a time-varying curvature instead of a distributed load. These replicates bending like an actual fish. Like the previous homework, the beam will be modeled as a discretized spring-node network. The integration would be implicit Euler method. To isolate and study how key parameters such as stiffness, actuation amplitude and frequency affect the pattern and bending deformation of the fish, different values of each parameter would be used to simulate the motion.

### IV. EXPECTED CONTRIBUTION

The goal of this project is to provide a straightforward, lightweight model of a soft robotic fish. Key parameters such as stiffness and actuation variables would be studied to reproduce the motion. With contents from M263F, this project will focus on using Euler-Bernoulli, implicit Euler and analysis of bending and stretching energy instead of full fluid computation requirement.

### V. IMPLEMENTATION

#### A. Overview

A 2D robotic fish swimming simulation is implemented using Euler-Bernoulli Beam simulation with time-varying actuation to generate fish-like motion. This fish is modeled as an elastic beam with spring-node networks consisting of 11 nodes undergoing deformation in a viscous fluid environment.

#### B. Geometry

Rod length:  $L = 0.1\text{m}$

Number of nodes  $nv = 11$

Discrete segment length:  $\Delta L = 0.01\text{m}$

Cross-sectional radius  $r_0 = 1\text{mm}$

Node radii  $R = \Delta L/10 = 1\text{mm}$

Middle node radius  $R_{mid} = 25\text{mm}$

#### C. Material Properties

Young's Modulus:  $Y = 1\text{Gpa}$

Bending Stiffness  $EI = 7.85 \times 10^{-7}\text{N/m}^2$

Axial Stiffness  $EA = 3.14 \times 10^3\text{N}$

Metal density  $\rho_{metal} = 7000\text{kg/m}^3$

#### D. Fluid Property

Fluid density  $\rho_{fluid} = 1000\text{kg/m}^3$

Fluid viscosity  $\mu = 5000\text{ Pas}$

#### E. Curvature Control

Swimming of the robotic fish is modeled as a time-varying of the natural curvature. The wave pattern is described as the function below:

$$\kappa_0(s, t) = A(s) \cdot r(t) \cdot \sin(2\pi f t - ks)$$

where

1.  $s$  is the arc length coordinate along the fish body
2.  $t$  is time
3.  $A$  is the amplitude of the motion
4.  $r$  is the smooth ramp-up function
5.  $f$  is the tail-beat frequency
6.  $k$  is the spatial wavenumber

The amplitude increases from head to tail as the envelope below:

$$A(s) = A_0 \left( 0.2 + 0.8 \frac{s}{L} \right),$$

which mimics the biological fish where the tail has larger motion than the head.

## F. Main Algorithm

**Algorithm 1** Robotic Fish Swimming Simulation

---

**Input:** Physical parameters ( $L, n_v, \Delta L, Y, \mu$ ), actuation parameters ( $A_0, f, k$ ), numerical parameters ( $\Delta t, t_{total}, tol$ )  
**Output:** Time series of fish configurations and diagnostics

- 1: **Initialize:**
- 2: Compute  $s_{bending} \leftarrow \text{linspace}(\Delta L, L - \Delta L, n_v - 2)$
- 3: Initialize positions  $q_0 \leftarrow [0, 0, \Delta L, 0, 2\Delta L, 0, \dots]^T$
- 4: Initialize velocities  $u_0 \leftarrow 0$
- 5: Build mass matrix  $M$ , damping matrix  $C$
- 6: Define boundary conditions:  $\text{fixed\_DOFs} \leftarrow [0, 1, 2, 3]$
- 7:
- 8:  $N_{steps} \leftarrow \lfloor t_{total}/\Delta t \rfloor$
- 9: **for**  $n = 1$  to  $N_{steps}$  **do**
- 10:    $t \leftarrow n \cdot \Delta t$
- 11:    $\kappa_0 \leftarrow \text{DesiredCurvature}(s_{bending}, t, A_0, f, k, t_{ramp})$
- 12:    $(q_{new}, flag) \leftarrow \text{ImplicitEulerStep}(q_0, u_0, \Delta t, \kappa_0, M, C)$
- 13:   **if**  $flag < 0$  **then**
- 14:     **break**
- 15:   **end if**
- 16:    $u_{new} \leftarrow (q_{new} - q_0)/\Delta t$
- 17:   Record diagnostics:  $y_{mid}[n], v_{mid}[n], \theta_{mid}[n]$
- 18:    $q_0 \leftarrow q_{new}, u_0 \leftarrow u_{new}$
- 19: **end for**
- 20: **return** Time series data

---

## VI. SINGLE SIMULATION

At this stage, the simulation reproduces fish-like swimming using a curvature-actuated Euler-Bernoulli beam model. The motion is generated by prescribed time-varying curvature and structural elasticity.

**Traveling Wave Propagation.** The wave travels down smoothly from the head toward the tail node like one on a real fish while maintaining a consistent wavelength and phase speed determined by the actuation frequency and spatial wavenumber.

**Amplitude Envelop Along the Body.** The deformation amplitude increases from head to tail as determined by the envelope function. This results in the oscillations become significantly larger as it getting closer to the tail.

**Qualitative Swimming Behavior.** Although full fluid-structure interaction is out of the scope of our project, oscillations still generate a visual swimming pattern. The tail demonstrates the largest lateral displacement, which is consistent with thrust-generating behavior in real fish.

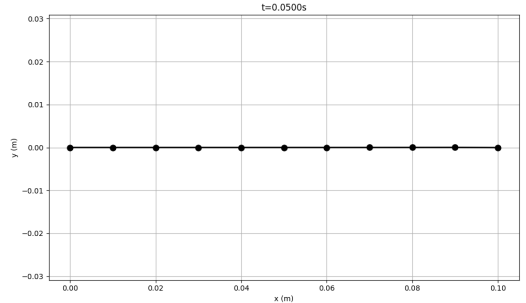


Figure 6 Tail Configuration at  $t = 0s$

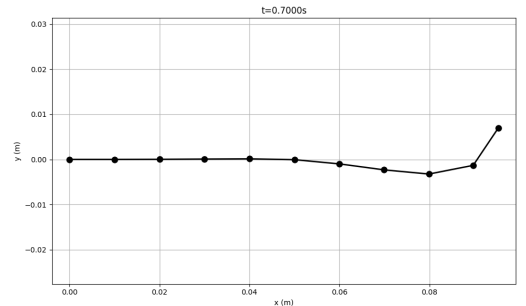


Figure 7 Tail Configuration at  $t = 0.7s$

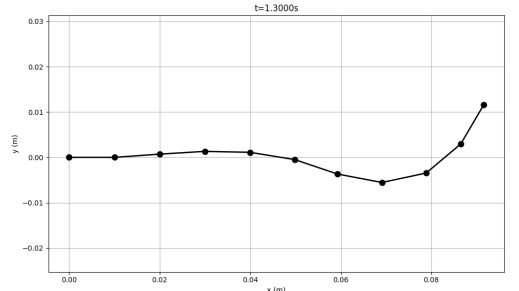


Figure 8 Tail Configuration at  $t = 1.3s$

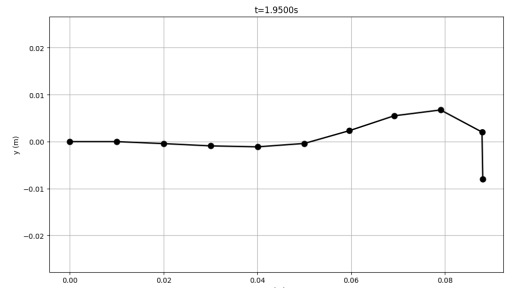


Figure 9 Tail Configuration at  $t = 1.95s$

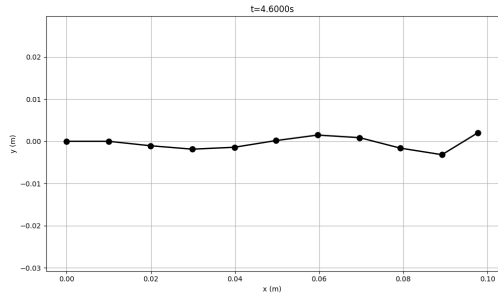


Figure 10 Tail Configuration at  $t = 4.6s$

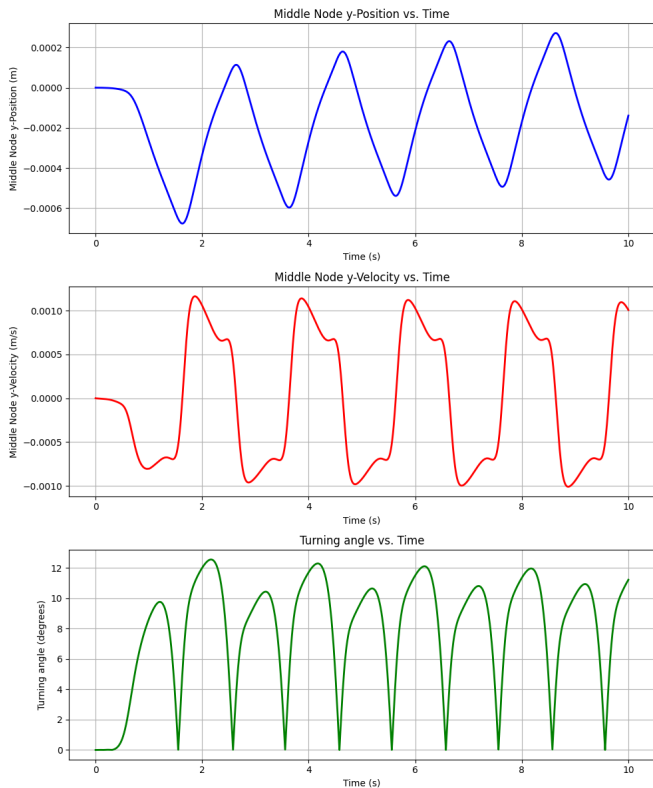


Figure 11 Middle Node y-position, y-velocity, y-turning angle vs time

## VII. PARAMETER SWEEP STUDY

To investigate how structural and actuation parameters affect the swimming kinematics of the soft robotic fish, a parameter sweep was conducted using the simulation framework. The goal of this sweep is to identify trends, and optimal operating regimes for propulsion.

A list of key parameters has been varied independently while keeping other parameters fixed at their baseline values. We changed the bending stiffness ( $EI$ ) to control the flexibility of the fish tail, the actuation amplitude ( $A$ ) to determine the magnitude of body curvature, actuation frequency ( $f$ ) to set the oscillation rate of the traveling rate, and the spatial wavenumber ( $k$ ) to control the number of wave cycles along the body. Each parameter was swept over

a physically reasonable range determined from the literature review and the limits of the implicit solver. For each sweep, we established a baseline simulation using the baseline values of all parameters, then we varied one parameter at a time across its specified range. At each parameter value, the system has been simulated until a steady state is reached. Lastly, the key performance metrics such as tail-tip lateral displacement, wave propagation speed, RMS deformation and maximum deformation to ensure consistent comparison across different parameter settings.

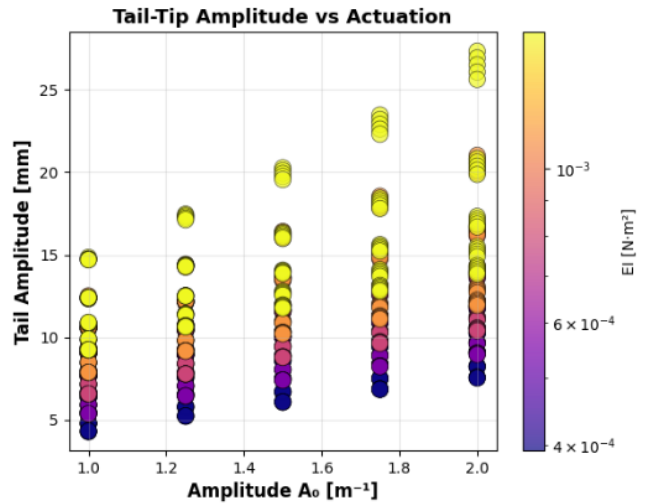


Figure 12 Tail-Tip Amplitude vs Actuation and Stiffness

**Tail-Tip Amplitude (4.29 – 27.33mm).** Large changes in tail amplitude indicates strong sensitivity to both bending stiffness and actuation amplitude. Higher stiffness or larger actuation amplitude tends to move results towards the higher range (~25-27mm), while lower stiffness or lower actuation input produces smaller amplitudes (~4-6mm). This reveals that higher stiffness may lead to rigid-like motion of the fish tail that results in larger tail-tip amplitude.

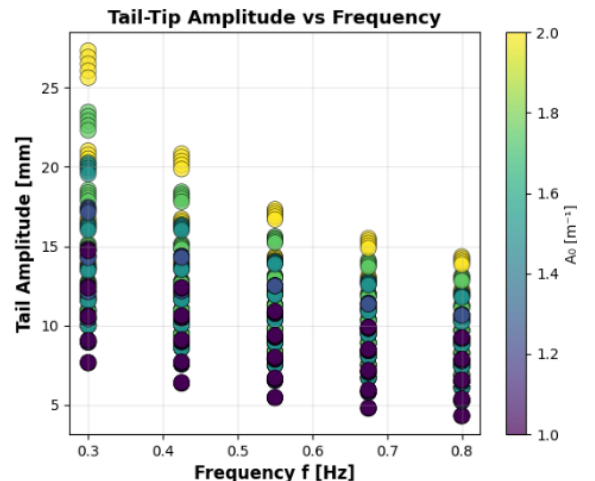


Figure 13 Tail-Tip vs Actuation Frequency

This plot reveals a significant inverse relationship between the actuation frequency and the resulting tail-tip amplitude. As the frequency increases from 0.3Hz to 0.8Hz, the maximum tail amplitude drops from over 27mm to 15mm, which suggests that at high oscillation rates, the viscous damping force of the beam's inertia prevents the tail from reaching higher deflection.

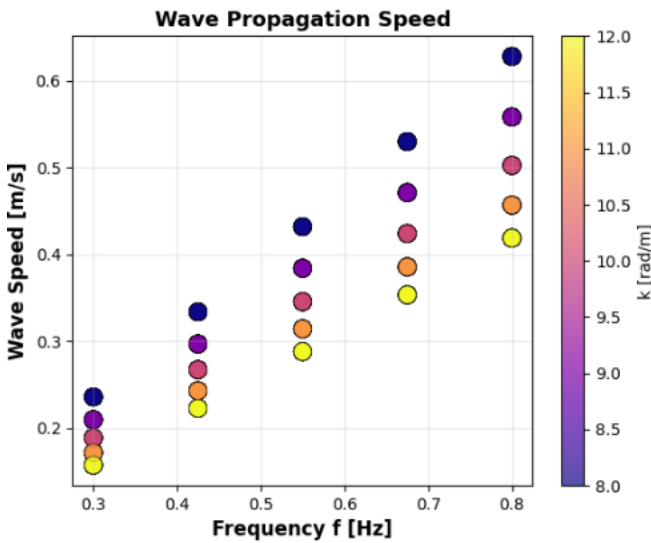


Figure 14 Wave Propagation Speed vs Actuation Frequency

**Wave Propagation (0.15m/s – 0.65m/s)** Wave speed increases with actuation frequency, as the traveling curvature wave travels faster along the tail. Speed increases from approximately 0.2m/s at 0.3Hz to over 0.6m/s at 0.8Hz, as higher actuation frequency drives a faster moving wave. For any fixed frequency, a higher spatial wavenumber  $k$  increases the wave propagation speed compared to a low one.

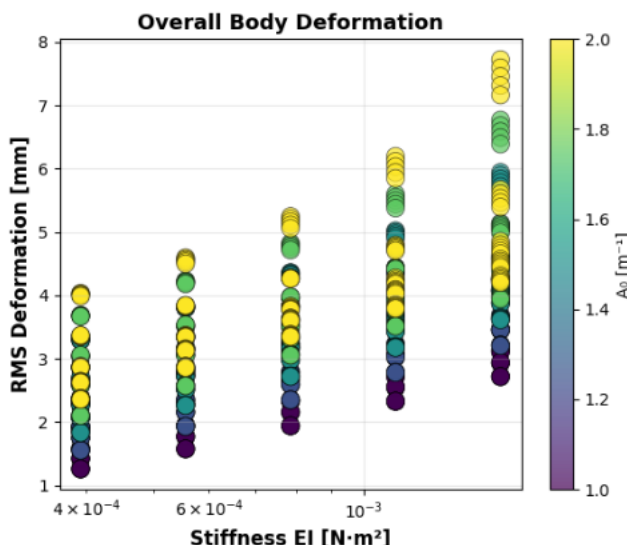


Figure 15 RMS Deformation vs Stiffness

RMS Deformation (1.32mm – 4.21mm) The effect of actuation amplitude is the strongest driver of overall deformation and has a positive relationship with the Root Mean Square deformation of the fish's tail. The RMS deformation also increases as the bending stiffness increases. This means a stiffer beam, when subjected to the same internal curvature actuation, results in a larger displacement, measured as the RMS deformation.

## VIII. CONCLUSION

This project implemented a discrete beam model to simulate the motion of a soft robotic fish under prescribed curvature. The simulation setup incorporated the classical node-spring network introduced in class to allow a simplified exploration of the coupled effects of material stiffness and actuation kinematics on swimming behavior. The results have demonstrated that the fish's deflection and tail displacement are highly sensitive to actuation amplitude, which suggests that it is the most important factor for a direct control mechanism. The illustrated relationship between wavenumber and wave speed also confirms the formula developed in wave theory.

## IX. FUTURE WORK

The current analysis focuses on the kinematic output of the swimming motion such as tail amplitude and deformation. To evaluate engineering utility of the soft robotic fish, future work would incorporate energy metrics to quantify efficiency. The next step is to calculate the conversion efficiency between the input (actuation and material parameters) and the output (kinematic energy). The primary energy generated by the prescribed natural curvature is stored as elastic bending energy in the beam. Calculating it requires integrating the moment applied by the actuation mechanism against the deformation. To quantify the output energy, a common metric would be the kinematic energy associated with a certain velocity of the fish generated by the natural curvature. The ultimate goal would be to perform a more focused parameter sweep to determine the parameter set that maximize the conversion between prescribed natural curvature and generated kinematic energy.

## REFERENCE

- [1] C. Eloy, “Optimal Strouhal number for swimming animals,” *Journal of Theoretical Biology*, vol. 324, pp. 41–49, 2012.
- [2] C. J. Esposito, J. L. Tangorra, B. E. Flammang, and G. V. Lauder, “A robotic fish caudal fin: Effects of stiffness and kinematics on locomotor performance,” *Journal of Experimental Biology*, vol. 215, no. 1, pp. 56–67, 2012.
- [3] R. K. Katzschatmann, J. DelPreto, R. MacCurdy, and D. Rus, “Exploration of underwater life with an acoustically controlled soft robotic fish,” *Science Robotics*, vol. 3, no. 16, p. eaar3449, 2018.
- [4] G. V. Lauder, P. G. Madden, R. Mittal, E. A. Jones, and T. V. Baker, “Fish-inspired robotics: Multi-phase hydrodynamics,” *Integrative and Comparative Biology*, vol. 52, no. 6, pp. 891–896, 2012.
- [5] J. Zhong, T. Wang, G. Li, and J. Zhu, “Tunable stiffness swimming robots,” *Science Robotics*, vol. 6, no. 54, p. eabd2971, 2021.
- [6] R. J. L. Badalamenti and M. S. Triantafyllou, “Passive robotic models of propulsion by the bodies and caudal fins of fish,” *Journal of Experimental Biology*, vol. 213, pp. 301–312, 2010. [Online]. Available: <https://www.researchgate.net/publication/228082613>
- [7] C. J. Esposito, J. L. Tangorra, B. E. Flammang, and G. V. Lauder, “A robotic fish caudal fin: Effects of stiffness and kinematics on locomotor performance,” *Journal of Experimental Biology*, vol. 215, no. 1, pp. 56–67, 2012. [Online]. Available: <https://journals.biologists.com/jeb/article/215/1/56/10790/>